Published in final edited form as:

FASEB J. 2024 January 31; 38(2): e23416. doi:10.1096/fj.202301393R.

Role of Ecto-5'-nucleotidase in Bladder Function

Sagar Barge[1,#], **Ali Wu**[1,#], **Lanlan Zhang**[1,#], **Simon C. Robson**[1,2], **Aria Olumi**[3], **Seth L. Alper**[1], **Mark L. Zeidel**[1], **Weiqun Yu**[1,*]

[1]Department of Medicine, Beth Israel Deaconess Medical Center and Harvard Medical School, Boston, Massachusetts

[2]Department of Anesthesia, Beth Israel Deaconess Medical Center and Harvard Medical School, Boston, Massachusetts

[3]Department of Surgery, Beth Israel Deaconess Medical Center and Harvard Medical School, Boston, Massachusetts

Abstract

Purinergic signaling plays an important role in regulating bladder contractility and voiding. Abnormal purinergic signaling is associated with lower urinary tract symptoms (LUTS). Ecto-5'-nucleotidase (NT5E) catalyzes dephosphorylation of extracellular AMP to adenosine, which in turn promotes adenosine-A2b receptor signaling to relax bladder smooth muscle (BSM). The functional importance of this mechanism was investigated using Nt5e knockout (Nt5eKO) mice. Increased voiding frequency of small voids revealed by voiding spot assay was corroborated by urodynamic studies showing shortened voiding intervals and decreased bladder compliance. Myography indicated reduced contractility of Nt5eKO BSM. These data support a role for NT5E in regulating bladder function through modulation of BSM contraction and relaxation. However, the abnormal bladder phenotype of Nt5eKO mice is much milder than we previously reported in A2b receptor knockout (A2bKO) mice, suggesting compensatory response(s) in Nt5eKO mouse bladder. To better understand this compensatory mechanism, we analyzed changes in purinergic and other receptors controlling BSM contraction and relaxation in the Nt5eKO bladder. We found that the relative abundance of muscarinic CHRM3, purinergic P2X1, and A2b receptors was unchanged; whereas P2Y12 receptor was significantly downregulated, suggesting a negative feedback response to elevated ADP signaling. Further studies of additional ecto-nucleotidases indicated significant upregulation of the nonspecific urothelial alkaline phosphatase ALPL, which might mitigate the degree of voiding dysfunction by compensating for Nt5e deletion. These data suggest a mechanistic complexity of the purinergic signaling network in bladder, and imply a

[*]Corresponding author: Weiqun Yu, Beth Israel Deaconess Medical Center, RN380B, 99 Brookline Avenue, Boston, MA 02215, Phone: 617-667-5842, wyu2@bidmc.harvard.edu.

[#]These authors contributed equally

Author Contributions

W. Y., L. Z., and A. W. performed voiding spot assay, W. Y. and L. Z. performed cystogram and myograph studies. A. W. and B. S. performed quantitative RT-PCR and Western blot, and analyzed data. B. S. performed enzymatic histochemistry, and analyzed data. W.Y. performed immunostaining & imaging. S.C.R., A.O., S.L.A., and M.L.Z. contributed to conception and interpretation of data. W.Y. conceived and supervised the project. W.Y. wrote the manuscript, and all authors critically discussed the results and reviewed the manuscript.

Competing interests

The authors declare no competing interests.

paracrine mechanism in which urothelium-released ATP and its rapidly produced metabolites coordinately regulate BSM contraction and relaxation.

Graphical Abstract

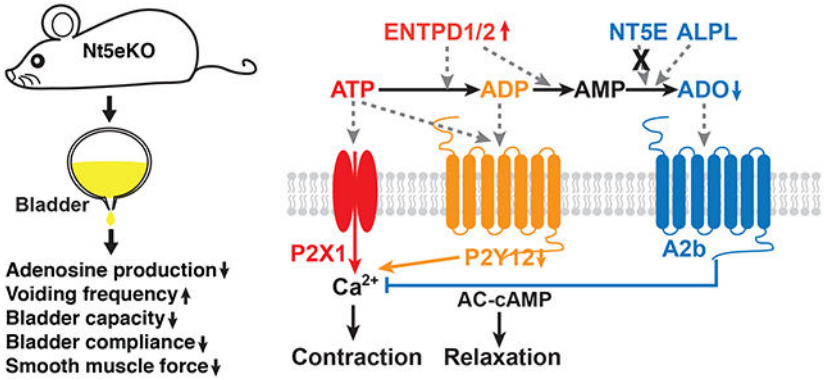

Nt5e knockout (Nt5eKO) mice exhibited increased voiding frequency of small voids. The bladder compliance is decreased with the voiding interval shortened. Bladder smooth muscle has decreased contractile forces. Mechanistically, deletion of Nt5e likely impaired the adenosine A2b receptor-mediated smooth muscle relaxation of the bladder. Significant compensatory changes of Alpl, Entpd1/2, and P2y12 were noticed which might mitigate the degree of voiding dysfunction in Nt5eKO mice. These data suggest a mechanistic complexity of the purinergic signaling network in the bladder, and imply that ATP and its rapidly produced metabolites coordinately regulate bladder contraction and relaxation.

Keywords

Lower urinary tract symptoms; Ecto-5’-nucleotidase; bladder smooth muscle; purinergic signaling; alkaline phosphatase

Introduction

Since the initial discovery more than 50 years ago of purinergic signaling as a modulator of urinary bladder contraction and relaxation (1), purinergic signaling is now known to play multiple roles in the regulation of bladder function. These roles include [1] a urothelial mechanosensory function in response to stretch-induced ATP release through connexin 43 (Cx43) hemi-channels, pannexin 1 (PANX1) channels and the vesicular nucleotide transporter, VNUT (2–4); [2] a P2X2/3 receptor-mediated afferent sensory function (5); [3] an adenosine receptor-mediated urothelial membrane trafficking function (6, 7); [4] a P2X1 receptor- and P2Y12 receptor-mediated bladder smooth muscle (BSM) contractile function (8–11); and [5] an adenosine A2b receptor-mediated BSM relaxation function (12). These and other recent advances indicate that purinergic signaling comprises a complex, dynamic, interactive network of signaling molecules including [1] the ligands ATP, ADP and adenosine (ADO); [2] purine-gated cation channels P2X1–7 and metabotropic purinergic G protein-coupled receptors P2Y1,2,4,6,11–14; P1 adenosine receptors (A1, A2a, A2b, A3); and [4] ecto-nucleoside triphosphate diphosphohydrolases ENTPD1, 2, 3, 8,

ecto-nucleotidases which sequentially convert extracellular ATP first to ADP and then to AMP. AMP is converted in turn to adenosine by ecto-5'-nucleotidase (NT5E) and urothelial alkaline phosphatase (ALPL). [5] Ecto-nucleotide pyrophosphatase/phosphodiesterase 1 and 3 (ENPP1 and ENPP3) of the bladder wall also contribute to the conversion of ATP to AMP (13, 14).

Although the mechanism by which this signaling network regulates bladder function remains incompletely understood, abnormal extracellular ATP levels (15, 16) and altered purinergic contractility (17–19) have been consistently reported in patients with lower urinary tract symptoms (LUTS). LUTS patients with overactive or obstructed bladders exhibit impaired ATP hydrolysis, with bladder contractility disproportionately sensitive to neuromuscular purinergic signaling as compared to normal bladders. These studies suggest that modulation of extracellular purine dynamics plays important roles in bladder function and dysfunction (15–21).

Our laboratory has determined that multiple ENTPDs are present within bladder wall, including predominant expression of ENTPD1 in BSM and vasculature, ENTPD2 in interstitial cells, ENTPD3 and alkaline phosphatase (ALPL) in urothelial cells, and NT5E in BSM (22). We have shown that urothelium can function as a mechanosensor to differentially release ATP in response to both the rate of change and magnitude of stretch (23, 24). We have found that urothelial ATP released into basolateral space is quickly converted by urothelial ENTPD3 and alkaline phosphatase (ALPL) into adenosine, which regulates bladder function through activation of multiple adenosine receptors (6, 24).

We also recently defined bladder wall P2Y12 as a major receptor for ADP, a contractile agonist of human bladder (25). We further determined that the adenosine A2b receptor plays a major role in BSM relaxation by inhibiting ATP- and ADP-mediated purinergic contraction (12). We have reported that the interplay of A2b and P2Y12 receptors through modulation of adenylyl cyclase (AC) – cAMP signaling can actively regulate bladder contractility (12). We showed that *P2y12* knockout (P2y12KO) mice exhibit a phenotype of increased bladder capacity, reduced voiding frequency, and increased BSM contractile force, whereas *Adora2b* knockout (A2bKO) mice have an overactive bladder with decreased capacity, increased voiding frequency, and reduced BSM contractile force. These studies further suggest the functional importance of purine interconversion enzymes in the regulation of bladder function.

However, little is known about the physiologic significance of purine interconversion enzymes in the bladder wall. We and others have previously reported that *Entpd1* knockout (Entpd1KO) mice exhibit abnormal extracellular purine kinetics in bladder wall which results in dysregulated BSM contractility (25, 26). We also demonstrated that BSM from Nt5e knockout (Nt5eKO) mice respond abnormally to ADP stimulation (25). As we previously demonstrated the importance of normal bladder function of signaling through the ADP receptor P2Y12 and adenosine receptor A2b, we hypothesized that NT5E conversion of AMP to adenosine in BSM might control bladder function by modulating BSM contraction and relaxation. Here, we have tested this hypothesis by investigating *in vivo* and *in vitro* bladder function in Nt5eKO mice.

Materials and Method

Materials.

Unless otherwise specified, all chemicals were obtained from Sigma (St. Louis, MO) and were of reagent grade or better. α,β-meATP was purchased from R&D system (Minneapolis, MN, USA).

Animals.

Both male and female C57BL/6J and Nt5eKO (B6.129S1-*Nt5e*^{tm1Lft}/J) mice (Jackson Laboratory, Bar Harbor, ME) aged 12–16 weeks old were used in this study. All animal studies were performed in adherence with U.S. National Institutes of Health guidelines for animal care and use and with the approval of the Beth Israel Deaconess Medical Center Institutional Animal Care and Use Committee (Protocol #: 026-2016, 010-2022). Mice were housed in standard polycarbonate cages and maintained on a 12:12-h light-dark cycle at 25°C with free access to food and water.

Nucleotidase histochemistry

A lead phosphate method was used to determine bladder tissue activities of ATPase, ADPase, and AMPase as previously described (26). Briefly, 6 μm tissue sections of 4 % paraformaldehyde-fixed male wild type and Nt5eKO bladders were preincubated with Tris-maleate sucrose buffer containing 0.25 M sucrose, 50mM tris maleate and 2mM $CaCl_2$ pH 7.4. for 30 min at room temperature. The enzymatic reactions were performed at 37°C for 60 min in TMS-buffered substrate solutions [2mM $Pb(NO_3)_2$, 5mM $MgCl_2$, 5 mM $MnCl_2$, and 3% dextran T250 (Sigma-Aldrich) containing 1 mM final concentrations of substrate: ATP, ADP or AMP (Sigma-Aldrich). Control sections were incubated in the absence of substrate. Lead orthophosphate precipitated by nucleotidase activity was visualized as brown deposits by incubating sections in 1% (v/v) $(NH_4)_2SO_3$ for 1 min. Sections were counterstained with hematoxylin and dehydrated in graded ethanol, mounted in Permount mounting medium (Fisher Scientific). Fixed, stained sections were imaged with an Olympus BX61 microscope. Staining intensity was quantified using ImageJ software (National Institutes of Health, Bethesda, MD, USA).

Voiding spot assay (VSA).

VSA (from ~10:00 A.M. to ~2:00 P.M.) was performed with both male and female mice, to determine the *in vivo* functional importance of Nt5e in regulating the bladder activity of both sexes. Individual mice were gently placed in a standard mouse cage with Blicks Cosmos Blotting Paper (Catalog no. 10422–1005) placed in the bottom for 4 h, during which time water was withheld and standard dry mouse chow was available. Mice were then returned to their home cages and the filter paper was recovered. Filters were imaged under ultraviolet light at 365nm in a UVP Chromato-Vue C-75 system (UVP, Upland, CA) with an onboard Canon digital single lens reflex camera (EOS Rebel T3, 12 megapixels). Overlapping voiding spots were visually examined and manually separated by outlining and copying, then pasting to a nearby empty space using ImageJ software (http://fiji.sc/wiki/index.php/Fiji). Images were analyzed by UrineQuant software (developed in collaboration

with the Harvard Imaging and Data Core). The results table containing the area of each individual voiding spot and the total number of spots, was imported into Excel for statistical analysis. A urine volume vs. area standard curve on this paper determined that a 1 mm^2 voiding spot represents 0.283 μl of urine. Voiding spots of area ≥ 80mm^2 were considered primary voiding spots (PVS), based on voiding spot patterns from hundreds of mice (27–29).

Cystometrogram (CMG).

CMGs were performed with PBS infusion (25 μl/min) as previously described in female mice (12, 30). Mice were anesthetized by subcutaneous injection of urethane (1.4 g/kg from 250 mg/ml solution in PBS) ~ 30 min before surgery. At the time of surgery, each mouse was further anesthetized with continuous flow isoflurane (3% induction, 1.0% maintenance). Once the pedal reflex was absent, a 1-cm midline abdominal incision was performed. Flame-flanged polyethylene-50 tubing sheathing a 25G x 1.5 in. needle was implanted through the dome of the bladder, then sutured in place (8-0 silk purse string). The incision site was sutured using sterile 5-0 silk, and each mouse was then placed into a Bollman mouse restrainer for 30–60 min stabilization. The catheter was connected to a pressure transducer (and syringe pump by side arm) coupled to data-acquisition devices (WPI Transbridge and AD Instruments Powerlab 4/35) and a computerized recording system (LabChart software). Bladder filling then commenced, after which voiding occurred naturally through the urethra. Repeated voiding cycles were assessed for change of voiding interval (time between peak pressures), basal pressure (minimum pressure after voiding), peak pressure (maximum voiding pressure minus basal pressure), and compliance (volume in μl required to increase pressure by one cm H_2O).

Myography.

Bladders from male mice were pinned on a small Sylgard block, and muscle was dissected free of the mucosal tissue. BSM strips were then cut longitudinally (2–3 mm wide and 5–7 mm long). Muscle strips were mounted in an SI-MB4 tissue bath system (World Precision Instruments, Sarasota, FL, USA). Force sensors were connected to a TBM 4M transbridge (World Precision Instruments), and the signal was amplified by PowerLab (AD Instruments, Colorado Springs, CO, USA) and monitored through Chart software (AD Instruments). BSM strips were gently pre-stretched to optimize contraction force, then pre-equilibrated for at least 1 h. All experiments were conducted at 37°C in a physiological saline solution containing (in mM) 120 NaCl, 5.9 KCl, 1.2 $MgCl_2$, 15.5 $NaHCO_3$, 1.2 NaH_2PO_4, 11.5 Glucose, and 2.5 mM $CaCl_2$, with continuous bubbling of 95% O_2 / 5% CO_2. Contraction force was sampled at 2000/s using Chart software. BSM tissue was subjected to electrical field stimulation (EFS) to mimic *in vivo* neurotransmitter release and to examine general BSM functionality. BSM strips were then treated with 10 μM atropine for 15 minutes to block muscarinic contractility, then subjected again to EFS to examine remaining purinergic contractility. P2X1 receptor-mediated purinergic contractility was further investigated by direct bladder stimulation with 10 μM P2X1 agonist α, β-meATP, which desensitizes cell surface receptors within 10–15 minutes. Finally, general BSM functionality was further examined in response to depolarization by 100 mM KCl.

Electrical field stimulation.

BSM strip EFS was carried out by a Grass S48 field stimulator (Grass Technologies, RI, USA) using standard protocols previously described: voltage was 50 V, stimulus duration was 0.05 ms, trains of stimuli lasted for 3 s at frequencies of 1, 2, 5, 10, 20, and 50 Hz (12, 30). Each stimulus was separated by 3-minute intervals (31). EFS-induced forces are sensitive to tetrodotoxin inhibition (32).

Quantitative RT-PCR.

Total RNA was extracted from bladders of female wild type and Nt5eKO mice using the RNeasy kit (Qiagen, Valencia, CA). First-strand cDNA was synthesized from 1 μg total RNA using a SuperScript III First-Strand Synthesis System (Invitrogen). RT-PCR for gene detection was performed with Bio-Rad T100 Thermal Cycler. Quantitative RT-PCR was performed using SYBR Green PCR Mix kits and a 7300 real-time PCR system (Applied Biosystems). *SDHA* (Succinate dehydrogenase complex, subunit A) was used as an internal control. Primer details are provided in Table 1.

Western blot analysis.

Rabbit anti-P2X1 antibody (1:1000, #APR-001; RRID: AB_2040052) was purchased from Alomone Labs (Jerusalem, Israel). Rabbit anti-Chrm3 antibody (1:1000, #PA5-77485; RRID: AB_2735644) was from Thermofisher Scientific (Waltham, MA USA). Sheep anti-Entpd1 (1:1000, #AF4398; RRID: AB_1061688), sheep anti-Entpd2 (1:1000, #AF5797; RRID: AB_10572702), goat anti-Alpl (1:1000, #AF2910; RRID: AB_664062), and sheep anti-Nt5e (1:1000, #AF4488; RRID: AB_951934) antibodies were from R&D system (Minneapolis, MN, USA). Bladder samples of male wild type and Nt5eKO mice were lysed in RIPA buffer (150 mM NaCl, 50 mM Tris, 1% v/v NP-40, 0.5% deoxycholic acid, and 0.1% w/v SDS, pH 7.4) containing protease inhibitors (Complete Mini; Roche Applied Science, Indianapolis, IN, USA). Proteins were separated by SDS-PAGE and transferred to PVDF membranes. Membranes were incubated with primary antibody at 4°C for 1 hour after overnight block with 5% non-fat milk. β-actin (Cell Signaling, 1:1000, #4967; RRID: AB_330288) was used as the internal control. Bands were visualized with Amersham ECL reagent (Arlington Heights, IL, USA). Exposed and developed film was scanned and image contrast corrected with Photoshop (Adobe Systems, San Jose, CA, USA). Images were imported into Adobe Illustrator CS4 (Adobe) for the generation of figures.

Immunofluorescence staining and microscopy imaging.

Excised bladders from female wild type and Nt5eKO mice were cut open longitudinally and fixed in 4% (wt/vol) paraformaldehyde in 100 mM sodium cacodylate buffer (pH 7.4) for 2 hours at room temperature. Fixed tissue was cryoprotected in Tissue-Plus™ O.C.T Compound, and was frozen on dry ice. Tissue was sectioned in a Cryostat microtome with a thickness of 5 μM, and then was blocked with 10% fetal bovine serum in PBS with 0.1% Triton X-100 for 30 min. Sections were then incubated with primary antibodies (1:100, sheep anti-Nt5e (1:1000, #AF4488; RRID: AB_951934)) in PBS overnight at 4°C. The anti-NT5E antibody was validated with tissue from Nt5eKO knockout mice (Figure 1). The sections were then incubated with Alexa Fluor 488–conjugated secondary antibody (diluted

1:100), and nuclei were stained with DAPI. Imaging was performed on an Olympus BX60 fluorescence microscope with a 40×/0.75 objective. Images (512 and 512 pixels) saved as TIFF files were imported into Adobe Illustrator CS4. Each bladder was sectioned to obtain 2 slides with approximately 4 sections of tissue on each slide. Each section was examined microscopically to ensure consistency of staining (22).

Statistical analyses.

The sample number in each experimental group contains a minimum of 4 based on our past experience with the proposed experimental design. Voiding spot assay required ≥10 animals in each group, due to the usually large standard deviation of PVS (primary voiding spot) number and size.

All data are expressed as means ± SD, or presented as boxes and whiskers (extending from minimum to maximum values). Data were analyzed by Student's *t*-test between two groups. If possible, a paired *t*-test was used. Bonferroni's multiple comparison post-hoc tests were used where necessary, and $P < 0.05$ was considered significant. At least 3 animals were used for myography studies. Each bladder usually yielded 3–4 valid muscle strips, and a nested t-test was used for the analysis of myographic experiments.

Results

Nt5eKO mice have altered ecto-nucleotidase activity in the bladder wall.

We previously discovered that NT5E is expressed only in BSM cells in the bladder wall (22). As shown in Figure 1, quantitative RT-PCR data indicate a dramatic reduction in *Nt5e* mRNA abundance (Figure 1A), in parallel with the complete disappearance of a ~75 kDa polypeptide in Nt5eKO bladder lysate samples (Figure 1B). The wild-type localization of Nt5e in BSM cell membrane is absent from BSM cells of Nt5eKO mice (Figure 1 C&D). These data confirm the loss of Nt5e expression in this animal model.

To evaluate how loss of NT5E expression affects bladder wall ecto-nucleotidase activity, we assessed enzyme activity by histochemistry with the lead phosphate method. Loss of Nt5e significantly decreased AMP hydrolysis activity in BSM, but not in lamina propria or in urothelium (Figure 2 C, F, &I). Interestingly, ATP hydrolysis activity in lamina propria of Nt5eKO bladder increased significantly (Figure 2 A, D, &G), suggesting compensatory ENTPD2 upregulation. ADP hydrolysis activity did not differ between wild-type and Nt5eKO bladders (Figure 2 B, E, and H).

Nt5eKO mice have altered voiding phenotype.

To understand the *in vivo* functional importance of NT5E on voiding phenotype, we performed VSA in both male and female Nt5eKO mice. As shown in Figure 3, Nt5eKO exhibited increased numbers of PVS per filter over 4 hours (female: 3.51 ± 1.27 (*wt:* mean±SD) vs. 4.45 ± 2.21 ($Nt5e^{-/-}$: mean±SD); male: 2.79 ± 1.57 (*wt:* mean±SD) vs. 4.03 ± 2.46 ($Nt5e^{-/-}$: mean±SD). Nt5eKO also exhibited reduced average PVS area (female: 366 ± 189 mm^2 (*wt:* mean±SD) vs. 318 ± 184 mm^2 ($Nt5e^{-/-}$: mean±SD); male: 560 ± 354 mm^2 (*wt:* mean±SD) vs. 465 ± 324 mm^2 ($Nt5e^{-/-}$: mean±SD)) (Fig. 3 A–D). Voiding

spots were further grouped according to area as shown in the frequency distribution graph in Figure 3F. > 50% (female) and ~ 40% (male) of individual Nt5eKO void spots exceed 300 mm^2 in area, greater than the corresponding wild type values of ~ 40% (female) and ~25% (male). However, the total voided volume over 4 hours is indistinguishable between wild type and Nt5eKO mice (Fig. 3E). These results showing increased void frequency and smaller void volume in Nt5eKO mice suggest a physiological role for NT5E in regulating bladder function. The similarly altered *in vivo* voiding phenotypes of male and female Nt5eKO mice were consistent with similar mechanisms in Nt5eKO bladders of both sexes. Therefore, subsequent mechanistic experiments were conducted in either male or female mice only.

Nt5eKO mice exhibit altered urodynamics.

CMG was performed on female wild type and Nt5eKO mice. As shown in Figure 4, wild type mice bladder-infused at 25 μL/min exhibited a voiding interval of ~4 minutes, whereas the Nt5eKO voiding interval was significantly reduced at 2–3 minutes (Figure 4 C). However, basal and peak pressures were each indistinguishable in wild type and Nt5eKO mice. As shown in Figure 4B for Nt5eKO mice, the rising curve at the filling stage is steeper than that of wild type mice (Figure 4A), reflecting decreased bladder compliance in Nt5eKO mice (Figure 4F). These urodynamic changes are consistent with the VSA data, supporting a phenotype of voiding frequency and small voids in Nt5eKO mice.

Nt5eKO mice have reduced smooth muscle contraction force.

Myogenic dysfunction can lead to altered voiding phenotype and urodynamics, and purinergic signaling is important to BSM contractility. Therefore, myograph studies were performed on isolated BSM strips to investigate the impact of NT5E deletion on BSM function. As shown in Figure 5 A–C, the contractile force of BSM strips increases in response to increased EFS frequency, mimicking *in vivo* BSM contraction in response to neurotransmitter release. BSM contraction force in *Nt5e*$^{-/-}$ mice BSM strips was significantly smaller than in wild type counterparts. To further confirm that the reduced contractile force was intrinsic to BSM, and not secondary to altered neurotransmitter release, BSM membrane potential was directly depolarized by exposure to elevated [KCl] to promote BSM contraction. KCl-treated BSM strips from *Nt5e*$^{-/-}$ bladders consistently exhibited lower contractile force than did similarly treated wild type BSM strips (Figure 5F). As noted above, bladder contraction is mediated mainly by parasympathetic co-release of ATP and acetylcholine (Ach), which respectively induce P2X1 receptor– and CHRM3 receptor–mediated signaling cascades. To examine possible changes in these signaling pathways in NT5E-deleted BSM, we tested bladder responses to the P2X1 receptor agonist α, β-meATP and to the muscarinic antagonist atropine. Contractile force in response to either α, β-meATP or to atropine and EFS was significantly reduced, suggesting significant alteration in purinergic signaling pathways in *Nt5e*$^{-/-}$ mouse bladder (Figure 5D & E).

Gene expression profiling of Nt5eKO mice indicates an altered purinergic signaling pathway.

To further understand the mechanism of impaired smooth muscle contractile function in *Nt5e*$^{-/-}$ mice, we measured the abundance of mRNAs encoding CHRM3 (M3 muscarinic

receptor) and purinergic pathway components involved in BSM contraction as shown in Table 1. Interestingly, levels of both CHRM3 and P2X1 mRNAs were statistically unchanged in *Nt5e*$^{-/-}$ mice bladders as compared to wild type controls. However, levels of ENTPD1, ENTPD2, and ALPL mRNAs (encoding enzymes that sequentially degrade ATP, ADP, AMP, and adenosine) were significantly higher in *Nt5e*$^{-/-}$ than in wild type mouse bladders. Although A2b mRNA level was unchanged, the level of mRNA encoding ADP receptor P2Y12 was significantly decreased.

As shown in Figure 6, expression levels of CHRM3 and P2X1 proteins were unchanged in *Nt5e*$^{-/-}$ mouse bladders, whereas expression of ENTPD1, ENTPD2, AND ALPL polypeptides was significantly increased in *Nt5e*$^{-/-}$ mouse bladders, consistent with corresponding changes in mRNA expression (Table 1). Using knockout animal models as negative controls (12), we were unable to find immunospecific antibodies for detection of P2Y12 or A2b receptor proteins, and so were unable to perform immunoblot studies of P2Y12 and A2b in *Nt5e*$^{-/-}$ mice bladders. These distinct expression changes of purinergic pathway components in response to NT5E deletion implicate a major contribution of altered purinergic pathways to dysregulated BSM contraction and voiding dysfunction.

Discussion

NT5E is the only enzyme expressed on the BSM surface that catalyzes the conversion of extracellular AMP to adenosine, a signaling molecule important for BSM relaxation (12, 22). Nt5eKO mice thus indeed exhibit a gross phenotype of voiding frequency and small voids (Figure 3). Urodynamic studies by CMG indicate a correspondingly shortened voiding interval and decreased bladder compliance (Figure 4). However, the voiding phenotype observed in Nt5eKO mice is much milder than the abnormality we have previously reported in the A2bKO mice model (12), in which mean PVS of ~ 6.3 voids in A2bKO mice substantially exceeded PVS of ~ 4.5 voids in Nt5eKO mice, and the A2bKO mean PVS area of ~260 mm^2 was much lower than the Nt5eKO mean PVS area of 321 mm^2 (12). The adenosine A2b receptor is a major adenosine receptor in BSM, and its activation can dramatically reduce voiding frequency and increase voided volume in mice. The discrepant phenotypes of Nt5eKO and A2bKO mice suggest a purinergic regulation of BSM contractility more complex than a simple Nt5e-catalyzed conversion of AMP to adenosine for local A2b receptor activation.

As with A2bKO mice, Nt5eKO mice bladder exhibit reduced contractile force in response to EFS, KCl, and α, β-meATP (Figure 5). However, bladder expression of both mRNAs and proteins encoding CHRM3 and P2X1, major receptors mediating BSM muscarinic and purinergic contractility, are indistinguishable from those in wild type animals (Figure 6), suggesting an intact BSM contractile machinery. What, then, might explain the reduced contractile force of Nt5eKO BSM strips compared to wild type BSM? Maximum smooth muscle contraction force requires optimized relaxation or elongation. Impaired smooth muscle relaxation (reduced elongation) or overstretch generates reduced maximum muscle contraction force (33). The reduced BSM contraction force in Nt5eKO bladders could reflect a lack of adenosine signaling-mediated BSM relaxation, as shown by decreased compliance (Figure 4). Although wild type and Nt5eKO mice BSM exhibit different contraction forces

(Figure 5), their basal and peak CMG pressures reveal no significant differences (Figure 4). This could be explained by Laplace's law (T=PR/2, where T = tension, reflecting muscle force, P = bladder pressure, R = bladder radius), such that even when pressures are equal in wild type and Nt5eKO mice bladders, the respective BSMs experience differential dynamic forces due to different values of R. As Nt5eKO bladders exhibit significant smaller voids, smaller R in Nt5eKO mice can be predicted, predicting a weaker BSM contraction force, as in the myography studies of Figure 5.

Interestingly, P2Y12 receptor mRNA expression was significantly decreased, whereas A2b receptor mRNA level was unchanged. As we have previously shown, the balance between P2Y12 and A2b receptor signaling through downstream adenylyl cyclase (AC) and the cAMP cascade is critical in regulating BSM relaxation and contraction, thereby modulating bladder storage and voiding function (12). We also previously demonstrated that ADP induced an extended contractile response in Nt5eKO mice bladders, which could contribute to the strain's abnormal voiding frequency phenotype (25). Thus, P2Y12 receptor-mediated signaling might be expected to play a dominant role in Nt5eKO bladders, compared to A2b receptor-mediated signaling. However, extended P2Y12 activation in Nt5eKO mice bladders might also desensitize surface P2Y12, causing negative feedback to BSM cells, as shown by decreased P2Y12 mRNA abundance (Table 1). Decreased P2Y12 receptor-mediated signaling increases bladder relaxation and compliance, as shown by the larger voids and decreased voiding frequency observed in P2y12KO mice (12). In the Nt5eKO mouse bladder, decreased P2Y12 receptor could shift the balance of P2y12 – A2b receptor signaling towards A2b signaling, thereby minimizing the Nt5eKO voiding frequency phenotype due to lack of adenosine. This compensatory mechanism in Nt5eKO mice could explain, at least in part, the milder voiding phenotype as compared to that of A2bKO mice.

We found robust upregulation of both mRNA and protein encoding ALPL, which converts AMP to adenosine in bladder wall (Table 1 and Figure 6). These mouse data are consistent with those from human patients with *Nt5e* loss-of-function mutations causing arterial calcifications with compensatory upregulation of ALPL, in whom treatment with adenosine reduced ALPL expression (34). However, ALPL in the bladder wall is not expressed on the surface of BSM cells, but rather in urothelial cells. ENTPD2, an ATPase expressed on interstitial cells, showed the 2nd largest upregulation in Nt5eKO mice bladders, while ENTPD1 - a BSM cell surface expressed ATPase was also upregulated. ATP and its metabolites are important signaling molecules regulating bladder function. During micturition, parasympathetic co-released ATP activates the P2X1 receptor to initiate BSM contraction for voiding. During the filling stage, the bladder wall undergoes continuously increased mechanical stretch by urine infusion from the kidney. Bladder urothelial cells are a major source of ATP release in the bladder wall. We and others have shown that urothelial-released ATP and its metabolites are finely regulated by stretch speed and magnitude, together with ecto-nucleotidase activity controlling temporally and spatially distinct kinetics of changes in concentrations of ATP and adenosine (6, 13, 14, 22, 24, 26). In Nt5eKO mouse bladder, urothelial-released ATP, ADP and AMP are likely increased due to lack of NT5E, which feeds back to upregulate expression of ALPL and ENTPD1/2. Consistent with this altered bladder wall expression of ecto-nucleotidase, enzymatic histochemistry studies

indicated significantly increased ATPase activity in lamina propria and decreased AMPase activity in the BSM layer of Nt5eKO bladders (Figure 2). The compensatory upregulation of ALPL and ENTPD1/2 therefore implies important roles for urothelial-released ATP and its metabolites in the balance between maintaining smooth muscle tone (P2Y12) to counteract wall tension, while simultaneously relaxing (elongating) BSM during the filling stage to accommodate influx of urine from the kidney.

This paracrine purinergic mechanism indicates the complexity of the purinergic network in the bladder wall, which might be another mechanism accounting for the milder phenotype observed in Nt5eKO mice (Figure 7). Comparably balanced mechanisms have been recognized in the cardiovascular system, such as the contribution of endothelial nitric oxide release to vascular smooth muscle relaxation while maintaining vascular tone (35, 36). However, little is known concerning such homeostatic functions in the bladder wall. Our study therefore suggests a paracrine pathway in which stretch-induced ATP release from urothelium is finely regulated by ecto-nucleotidases to produce the agonists ADP and adenosine, which diffuse through the underlying interstitial space to modulate bladder muscle tone and contractility (37). Additional mechanisms may also account for the much milder bladder phenotype of Nt5eKO mice as compared to that of A2bKO mice. One such mechanism may involve adenosine transporter-mediated intracellular adenosine efflux into the extracellular space (38), a possibility requiring further investigation.

In summary, Nt5eKO mice exhibit increased voiding frequency and small voids with reduced BSM contraction force. Molecular studies indicate compensatory regulation of purinergic enzymes and receptors which partially mitigate the voiding dysfunction induced by deletion of NT5E. The distinct patterns of change exhibited by these mRNAs and proteins suggest an interesting urothelial paracrine pathway that regulates BSM function (Figure 7), as shown in a previous *in vitro* organ bath study (37). These data indicate an important role of urothelial purinergic signaling in controlling bladder contraction and relaxation. Future in-depth studies on the role of other ecto-nucleotidases in the modulation of bladder function will be required. A better understanding of purinergic regulation of bladder function should facilitate improved therapeutic strategies to treat LUTS patients.

Acknowledgments

The authors acknowledge funding received from National Institute on Diabetes and Digestive and Kidney Diseases/ National Institutes of Health grant K99/R00 DK095922 and R01 DK126674 (W.Y).

Data availability Statement

The datasets used and analyzed during the current study are available from the corresponding author on reasonable request.

References

1. Burnstock G, Satchell DG, and Smythe A (1972) A comparison of the excitatory and inhibitory effects of non-adrenergic, non-cholinergic nerve stimulation and exogenously applied ATP on a variety of smooth muscle preparations from different vertebrate species. Br J Pharmacol 46, 234–242 [PubMed: 4631338]

2. Negoro H, Kanematsu A, Doi M, Suadicani SO, Matsuo M, Imamura M, Okinami T, Nishikawa N, Oura T, Matsui S, Seo K, Tainaka M, Urabe S, Kiyokage E, Todo T, Okamura H, Tabata Y, and Ogawa O (2012) Involvement of urinary bladder Connexin43 and the circadian clock in coordination of diurnal micturition rhythm. Nat Commun 3, 809 [PubMed: 22549838]

3. Negoro H, Urban-Maldonado M, Liou LS, Spray DC, Thi MM, and Suadicani SO (2014) Pannexin 1 channels play essential roles in urothelial mechanotransduction and intercellular signaling. PloS one 9, e106269 [PubMed: 25170954]

4. Nakagomi H, Yoshiyama M, Mochizuki T, Miyamoto T, Komatsu R, Imura Y, Morizawa Y, Hiasa M, Miyaji T, Kira S, Araki I, Fujishita K, Shibata K, Shigetomi E, Shinozaki Y, Ichikawa R, Uneyama H, Iwatsuki K, Nomura M, de Groat WC, Moriyama Y, Takeda M, and Koizumi S (2016) Urothelial ATP exocytosis: regulation of bladder compliance in the urine storage phase. Sci Rep 6, 29761 [PubMed: 27412485]

5. Cockayne DA, Dunn PM, Zhong Y, Rong W, Hamilton SG, Knight GE, Ruan HZ, Ma B, Yip P, Nunn P, McMahon SB, Burnstock G, and Ford AP (2005) P2X2 knockout mice and P2X2/P2X3 double knockout mice reveal a role for the P2X2 receptor subunit in mediating multiple sensory effects of ATP. J Physiol 567, 621–639 [PubMed: 15961431]

6. Yu W, Zacharia LC, Jackson EK, and Apodaca G (2006) Adenosine receptor expression and function in bladder uroepithelium. American journal of physiology. Cell physiology 291, C254–265 [PubMed: 16571869]

7. Prakasam HS, Gallo LI, Li H, Ruiz WG, Hallows KR, and Apodaca G (2014) A1 adenosine receptor-stimulated exocytosis in bladder umbrella cells requires phosphorylation of ADAM17 Ser-811 and EGF receptor transactivation. Mol Biol Cell 25, 3798–3812 [PubMed: 25232008]

8. Mulryan K, Gitterman DP, Lewis CJ, Vial C, Leckie BJ, Cobb AL, Brown JE, Conley EC, Buell G, Pritchard CA, and Evans RJ (2000) Reduced vas deferens contraction and male infertility in mice lacking P2X1 receptors. Nature 403, 86–89 [PubMed: 10638758]

9. Vial C, and Evans RJ (2000) P2X receptor expression in mouse urinary bladder and the requirement of P2X(1) receptors for functional P2X receptor responses in the mouse urinary bladder smooth muscle. Br J Pharmacol 131, 1489–1495 [PubMed: 11090125]

10. Palea S, Corsi M, Pietra C, Artibani W, Calpista A, Gaviraghi G, and Trist DG (1994) ADP beta S induces contraction of the human isolated urinary bladder through a purinoceptor subtype different from P2X and P2Y. J Pharmacol Exp Ther 269, 193–197 [PubMed: 8169824]

11. Burnstock G, Cusack NJ, and Meldrum LA (1984) Effects of phosphorothioate analogues of ATP, ADP and AMP on guinea-pig taenia coli and urinary bladder. Br J Pharmacol 82, 369–374 [PubMed: 6733363]

12. Hao Y, Wang L, Chen H, Hill WG, Robson SC, Zeidel ML, and Yu W (2019) Targetable purinergic receptors P2Y12 and A2b antagonistically regulate bladder function. JCI Insight 4

13. Aresta Branco MSL, Gutierrez Cruz A, Dayton J, Perrino BA, and Mutafova-Yambolieva VN (2022) Mechanosensitive Hydrolysis of ATP and ADP in Lamina Propria of the Murine Bladder by Membrane-Bound and Soluble Nucleotidases. Front Physiol 13, 918100 [PubMed: 35784885]

14. Gutierrez Cruz A, Aresta Branco MSL, Perrino BA, Sanders KM, and Mutafova-Yambolieva VN (2022) Urinary ATP Levels Are Controlled by Nucleotidases Released from the Urothelium in a Regulated Manner. Metabolites 13

15. Silva-Ramos M, Silva I, Faria M, Magalhaes-Cardoso MT, Correia J, Ferreirinha F, and Correia-de-Sa P (2015) Impairment of ATP hydrolysis decreases adenosine A1 receptor tonus favoring cholinergic nerve hyperactivity in the obstructed human urinary bladder. Purinergic Signal 11, 595–606 [PubMed: 26521170]

16. Nardi-Schreiber A, Sapir G, Gamliel A, Kakhlon O, Sosna J, Gomori JM, Meiner V, Lossos A, and Katz-Brull R (2017) Defective ATP breakdown activity related to an ENTPD1 gene mutation demonstrated using (31)P NMR spectroscopy. Chem Commun (Camb) 53, 9121–9124 [PubMed: 28759073]

17. Palea S, Artibani W, Ostardo E, Trist DG, and Pietra C (1993) Evidence for purinergic neurotransmission in human urinary bladder affected by interstitial cystitis. J Urol 150, 2007–2012 [PubMed: 8230554]

18. Saito M, Kondo A, Kato T, Hasegawa S, and Miyake K (1993) Response of the human neurogenic bladder to KCl, carbachol, ATP and CaCl2. Br J Urol 72, 298–302 [PubMed: 8220990]
19. Harvey RA, Skennerton DE, Newgreen D, and Fry CH (2002) The contractile potency of adenosine triphosphate and ecto-adenosine triphosphatase activity in guinea pig detrusor and detrusor from patients with a stable, unstable or obstructed bladder. J Urol 168, 1235–1239 [PubMed: 12187274]
20. Ouslander JG (2004) Management of overactive bladder. N Engl J Med 350, 786–799 [PubMed: 14973214]
21. Burnstock G (2014) Purinergic signalling in the urinary tract in health and disease. Purinergic Signal 10, 103–155 [PubMed: 24265069]
22. Yu W, Robson SC, and Hill WG (2011) Expression and distribution of ectonucleotidases in mouse urinary bladder. PloS one 6, e18704 [PubMed: 21533188]
23. Yu W, Khandelwal P, and Apodaca G (2009) Distinct apical and basolateral membrane requirements for stretch-induced membrane traffic at the apical surface of bladder umbrella cells. Mol Biol Cell 20, 282–295 [PubMed: 18987341]
24. Yu W (2015) Polarized ATP distribution in urothelial mucosal and serosal space is differentially regulated by stretch and ectonucleotidases. Am J Physiol Renal Physiol 309, F864–872 [PubMed: 26336160]
25. Yu W, Sun X, Robson SC, and Hill WG (2014) ADP-induced bladder contractility is mediated by P2Y12 receptor and temporally regulated by ectonucleotidases and adenosine signaling. FASEB J
26. Babou Kammoe RB, Kauffenstein G, Pelletier J, Robaye B, and Sevigny J (2021) NTPDase1 Modulates Smooth Muscle Contraction in Mice Bladder by Regulating Nucleotide Receptor Activation Distinctly in Male and Female. Biomolecules 11
27. Chen H, Zhang L, Hill WG, and Yu W (2017) Evaluating the voiding spot assay in mice: a simple method with complex environmental interactions. Am J Physiol Renal Physiol 313, F1274–F1280 [PubMed: 28835420]
28. Yu W, Ackert-Bicknell C, Larigakis JD, MacIver B, Steers WD, Churchill GA, Hill WG, and Zeidel ML (2014) Spontaneous voiding by mice reveals strain-specific lower urinary tract function to be a quantitative genetic trait. Am J Physiol Renal Physiol 306, F1296–1307 [PubMed: 24717733]
29. Rajandram R, Ong TA, Razack AH, MacIver B, Zeidel M, and Yu W (2016) Intact urothelial barrier function in a mouse model of ketamine-induced voiding dysfunction. Am J Physiol Renal Physiol 310, F885–894 [PubMed: 26911853]
30. Chen H, Vandorpe DH, Xie X, Alper SL, Zeidel ML, and Yu W (2020) Disruption of Cav1.2-mediated signaling is a pathway for ketamine-induced pathology. Nat Commun 11, 4328 [PubMed: 32859919]
31. Yu W, Sun X, Robson SC, and Hill WG (2013) Extracellular UDP enhances P2X-mediated bladder smooth muscle contractility via P2Y(6) activation of the phospholipase C/inositol trisphosphate pathway. FASEB J 27, 1895–1903 [PubMed: 23362118]
32. Yu W, Sun X, Robson SC, and Hill WG (2013) Extracellular UDP enhances P2X-mediated bladder smooth muscle contractility via P2Y6 activation of the phospholipase C/inositol trisphosphate pathway. FASEB J 27, 1895–1903 [PubMed: 23362118]
33. Uvelius B, and Gabella G (1980) Relation between cell length and force production in urinary bladder smooth muscle. Acta Physiol Scand 110, 357–365 [PubMed: 7234441]
34. St Hilaire C, Ziegler SG, Markello TC, Brusco A, Groden C, Gill F, Carlson-Donohoe H, Lederman RJ, Chen MY, Yang D, Siegenthaler MP, Arduino C, Mancini C, Freudenthal B, Stanescu HC, Zdebik AA, Chaganti RK, Nussbaum RL, Kleta R, Gahl WA, and Boehm M (2011) NT5E mutations and arterial calcifications. N Engl J Med 364, 432–442 [PubMed: 21288095]
35. Lu LF, and Fiscus RR (1999) Nitric oxide donors enhance calcitonin gene-related peptide-induced elevations of cyclic AMP in vascular smooth muscle cells. Eur J Pharmacol 376, 307–314 [PubMed: 10448892]
36. Grange RW, Isotani E, Lau KS, Kamm KE, Huang PL, and Stull JT (2001) Nitric oxide contributes to vascular smooth muscle relaxation in contracting fast-twitch muscles. Physiol Genomics 5, 35–44 [PubMed: 11161004]

37. Sui G, Fry CH, Montgomery B, Roberts M, Wu R, and Wu C (2014) Purinergic and muscarinic modulation of ATP release from the urothelium and its paracrine actions. Am J Physiol Renal Physiol 306, F286–298 [PubMed: 24285497]

38. Pastor-Anglada M, and Perez-Torras S (2018) Who Is Who in Adenosine Transport. Front Pharmacol 9, 627 [PubMed: 29962948]

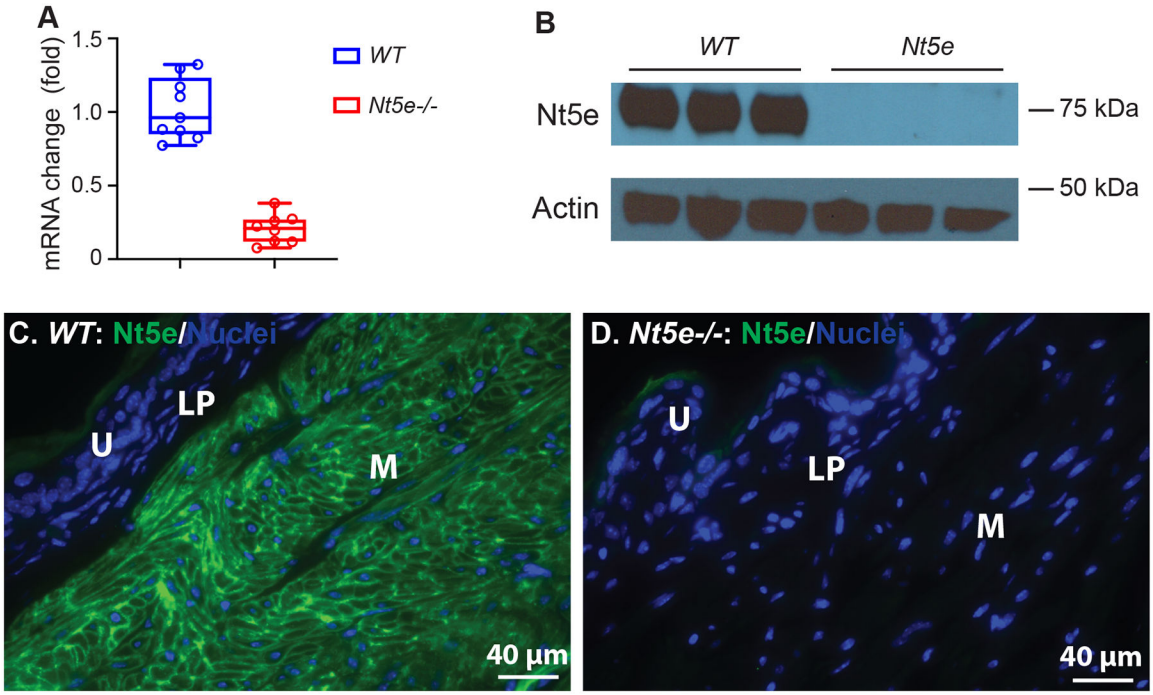

Figure 1. Nt5eKO mouse bladder lacks Nt5e expression.

Wild type and Nt5eKO mice bladders were analyzed by quantitative RT-PCR (A) and Western blot (B), indicating deletion of Nt5e in BSM. Actin gene and protein were used for normalization of quantitative RT-PCR (A) and Western blot (B). Wild type bladder labeled with specific anti-Nt5e antibody revealed strong immunofluorescence on BSM membrane (green in the panel C), but staining was undetected in Nt5eKO BSM cells (D). Nuclei were stained with DAPI (blue). U: urothelium; LP: lamina propria; M: smooth muscle. Data were analyzed by unpaired, two-tailed Student *t*-test. *: $p < 0.05$.

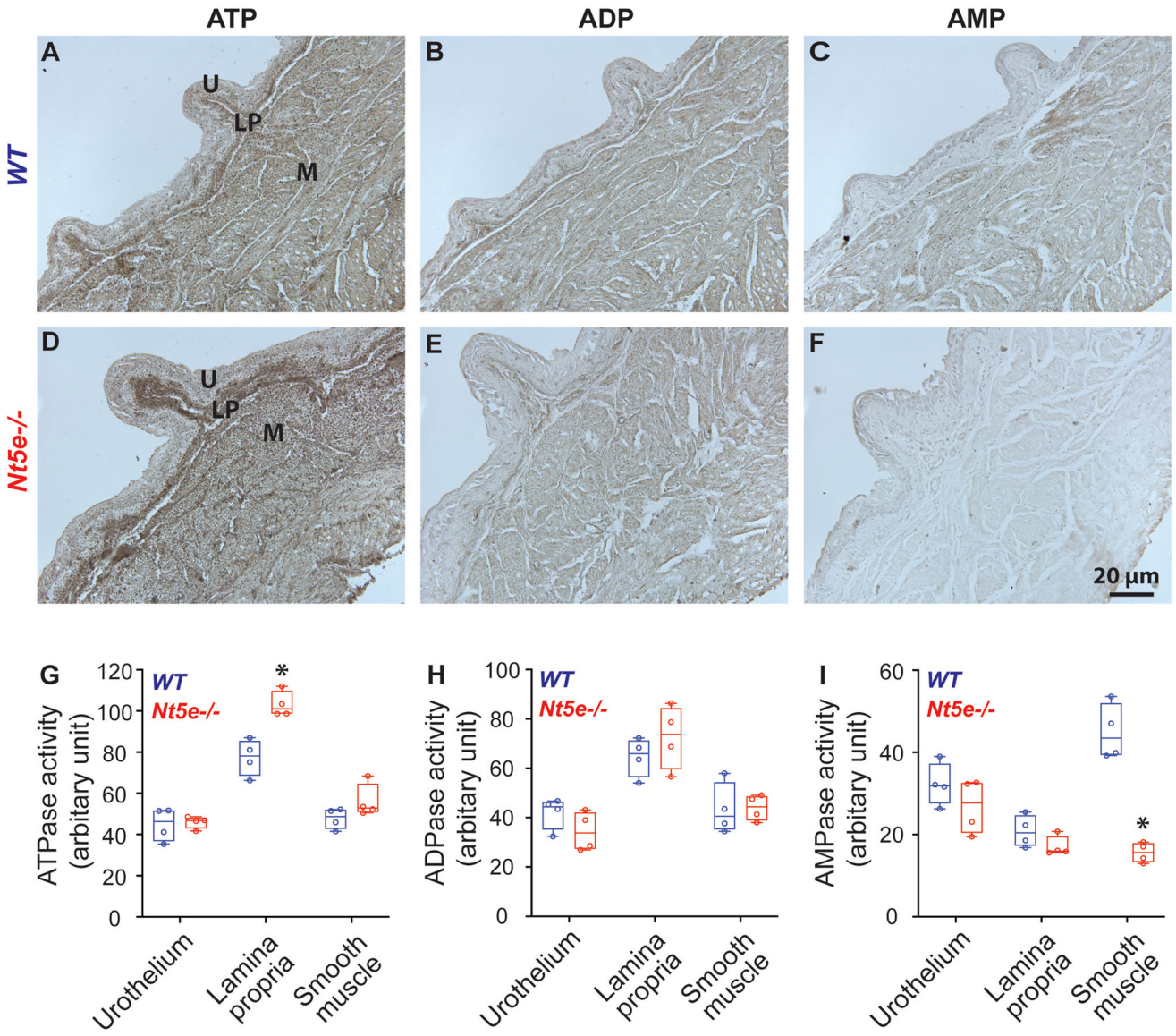

Figure 2. Nt5eKO mouse bladder exhibits altered ecto-nucleotidase activity.

A lead phosphate method was used to determine ATPase, ADPase, and AMPase activities in bladders of wild type (A–C, n=4) and Nt5eKO mice (D–F, n=4). U: urothelium; LP: lamina propria; M: smooth muscle. Quantitated data are shown as (G-I). Data are shown as boxes and whiskers, with centerline indicating median, boxes encompassing 75% of the data, and whiskers marking minimum and maximum values. Data were analyzed by unpaired, two-tailed Student *t*-test. *: $p < 0.05$.

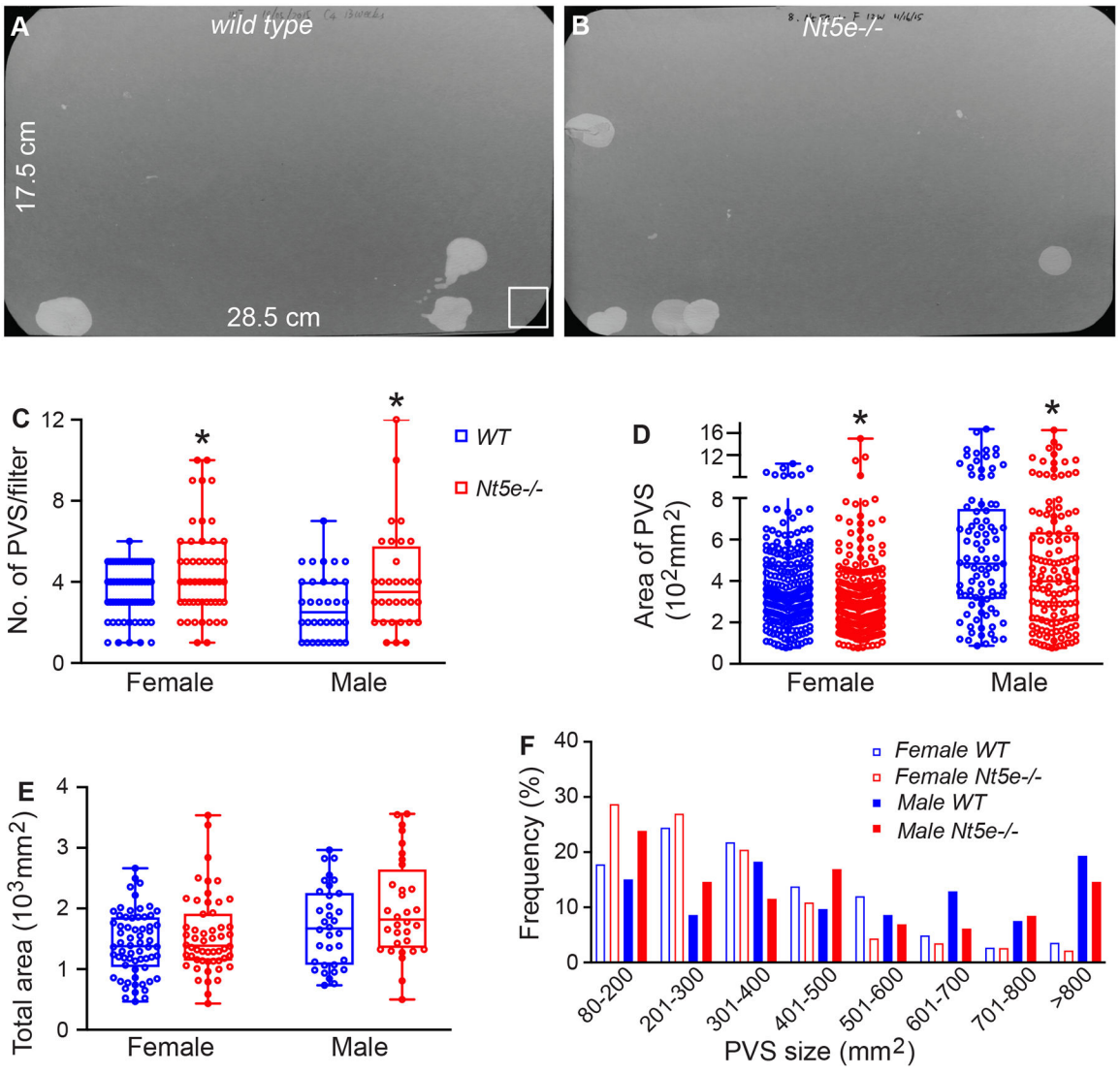

Figure 3. Nt5eKO mice have altered voiding phenotype.

(A&B) Representative filters show UV–illuminated urine spots from *WT* (A, female n=64, male n=34) and *Nt5eKO* mice (B, female n=51, male n=32). (C–E) Summary data of PVS number (C), PVS area (D), and total area of voiding spots per filter (E). (F) Frequency distribution graph of spot area. Data are shown as boxes and whiskers. Data were analyzed using the unpaired, two-tailed Student *t*-test with two tails. *: $p < 0.05$.

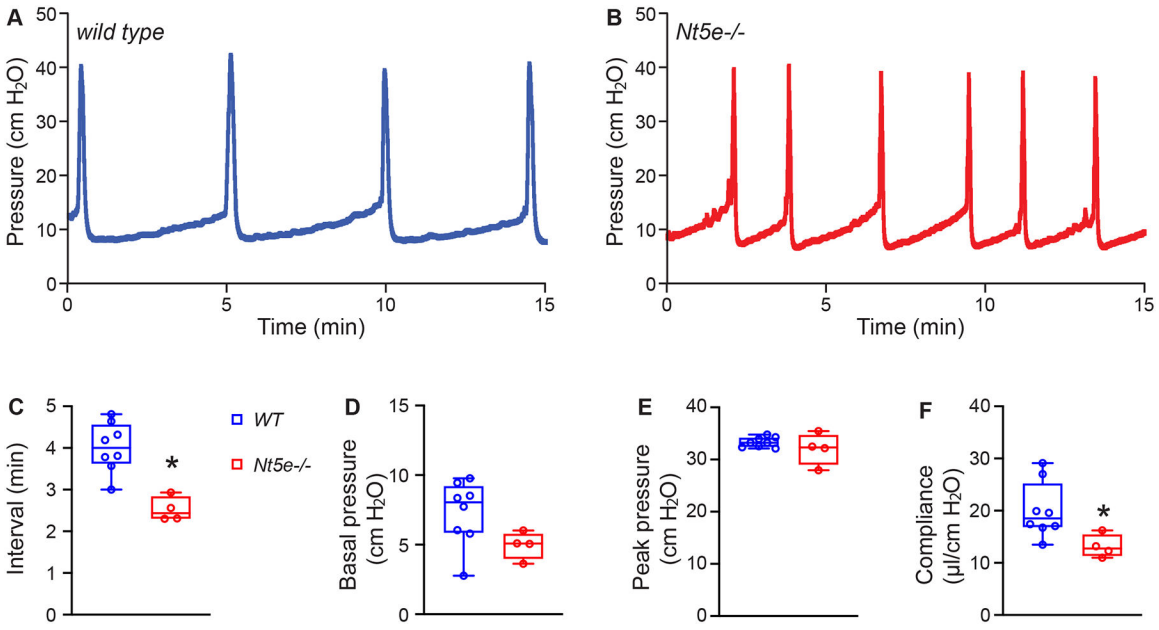

Figure 4. Nt5eKO mice exhibit altered urodynamics.

(A&B) Representative CMG traces from female *WT* (A, n=8) and *Nt5eKO* (B, n=4) mice. (C–F) Summarized urodynamic data from CMGs showing voiding interval (C), basal pressure (D), peak pressure (E), and compliance (F). Data are shown as boxes and whiskers. Data were analyzed using the unpaired, two-tailed Student *t*-test. *: $p < 0.05$.

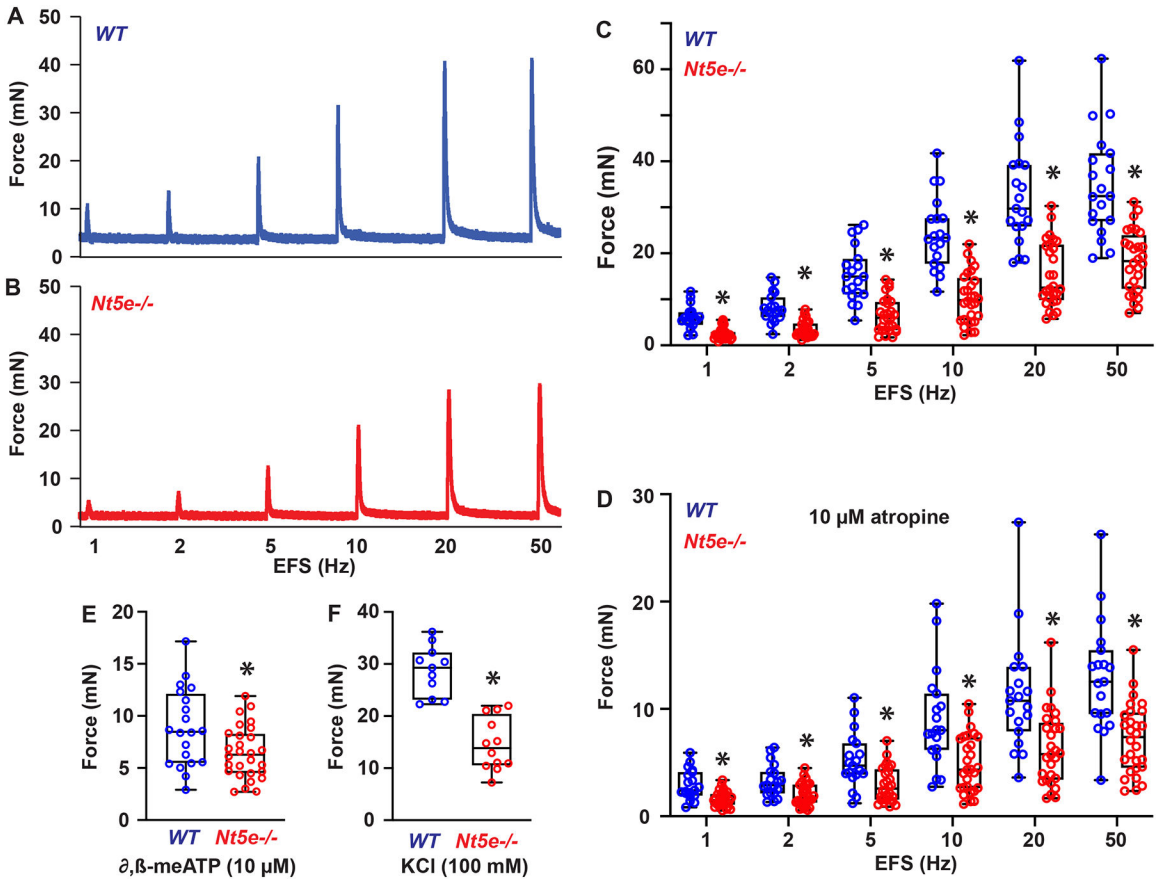

Figure 5. Nt5eKO mice have reduced smooth muscle contraction force.

(A&B) Representative traces of EFS-induced BSM contraction from male *WT* (A, n=20 strips from 5 mice) and *Nt5eKO* mice (B, n=28 strips from 7 mice) in response to EFS, with summarized data presented in (C). (D) summarized data of purinergic BSM contraction force assessed by EFS in the presence of atropine inhibition. (E&F) Summarized data of BSM contraction force in response to α, β-meATP (E, n=20 strips from 5 mice for WT*, and* n=28 strips from 7 mice for Nt5eKO) and KCl (F, n=11 strips from 3 mice for WT, and n=12 strips from 3 mice for Nt5eKO) stimuli. Data are shown as boxes and whiskers. Data were analyzed using the nested unpaired, two-tailed Student *t*-test. *: $p < 0.05$.

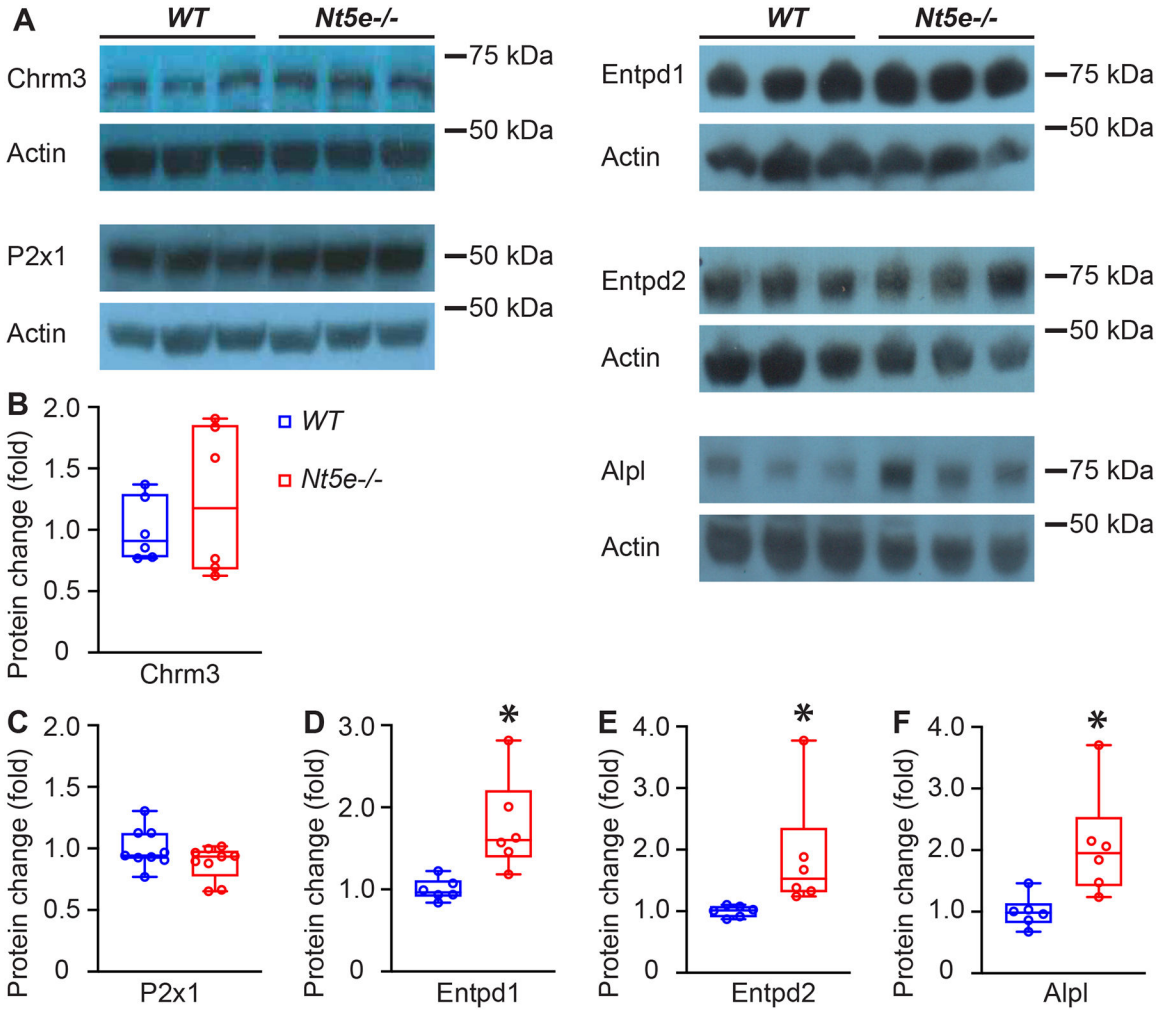

Figure 6.

Altered protein expression contributes to the voiding phenotype in Nt5eKO mouse bladders. (A) Western blot of CHRM3, P2X1, ENTPD1, ENTPD2, and ALPL proteins from WT (n=6) and Nt5eKO mice bladders (n=6). β actin was used as loading control for normalization, and quantitated data are shown as (B-F). Data are shown as boxes and whiskers. Data were analyzed using the unpaired, two-tailed Student *t*-test. *: $p < 0.05$.

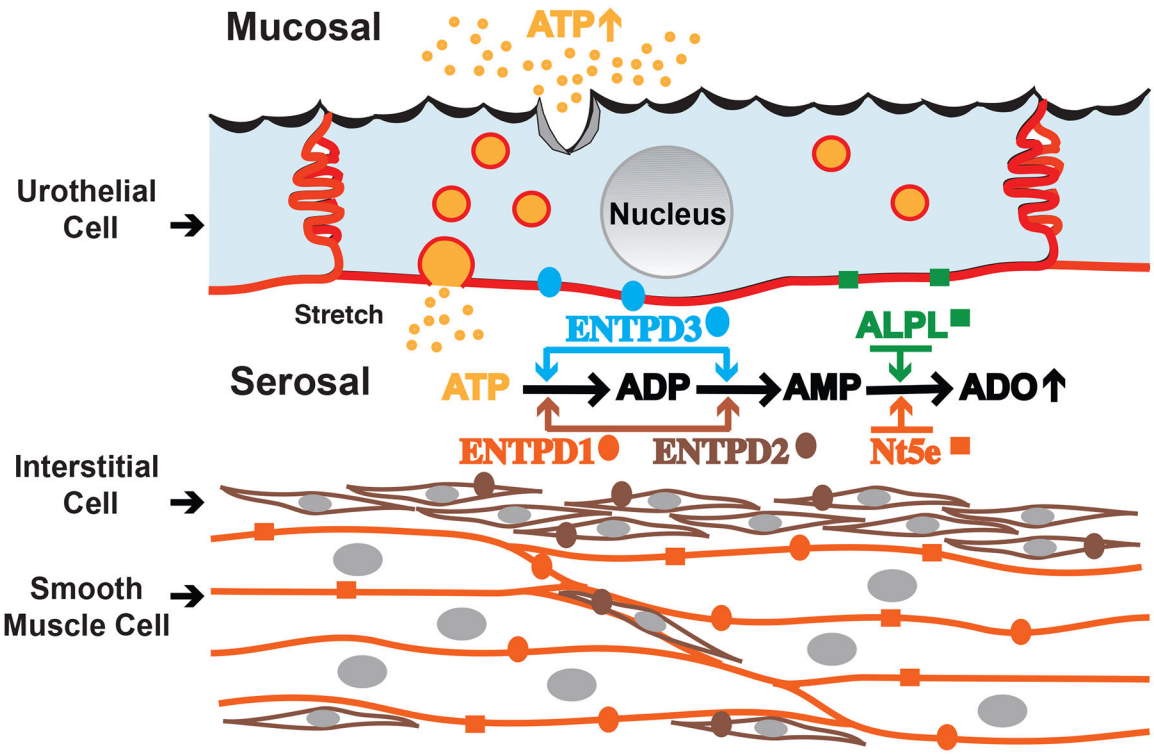

Figure 7.

Proposed model for regulation of urothelial ATP release, metabolism, and paracrine function. During bladder filling stage, stretch induces urothelial ATP release. Released ATP can be sequentially converted into ADP, AMP and adenosine by local urothelial ENTPD3 and ALPL. ATP, ADP and adenosine can diffuse further into the lamina propria and BSM layer, where they undergo metabolism by ENTPD1, ENTPD2, and Nt5e. Fine tuning of ATP release kinetics and its metabolism to ADP, AMP and adenosine are important for regulation of BSM tone through activation of purinergic receptors of P2X1, P2Y12, and A2b. Deletion of *Nt5e* causes feedback upregulation of ALPL to increase conversion of AMP to adenosine, as well as upregulation of other ENTPDs to increase ATP metabolism.

Table 1.

Quantitative RT-PCR results for some purinergic genes in *Nt5e*$^{-/-}$ bladders. Data are analyzed by unpaired, two-tailed Student *t*-tests, and are shown as means +/− standard deviation from (n) mice.

Gene	Primers	*Wild type* (n)	*Nt5e*$^{-/-}$ (n)
Nt5e	F: GTCCATGTGCATTGTAAACGG R: AGGTCAAATGTCCCTCCAAAG	1.02 ± 0.20 (9)	0.21 ± 0.10 (8) *
Entpd1	F: CTCTGCAATTCCGTCTCTATGG R: TGGGTTAAAGCATGGGTCC	1.00 ± 0.10 (12)	1.19 ± 0.23 (12) *
Entpd2	F: CGTCTCTGGGCTCTTCAATATC R: CCATCACTGTCTTCAGGAAGTC	1.00 ± 0.07 (6)	1.79 ± 0.13 (6) *
Alpl	F: CAGGCCGCCTTCATAAGCA R: GTTAATTGACGTTCCGATCCTGC	1.01 ± 0.15 (6)	2.00 ± 0.65 (5) *
P2rx1	F: TGGGAGTCATTTTCCGTCTG R: TGCTGATAAGGCCACTTGAG	1.03 ± 0.10 (8)	0.95 ± 0.17 (9)
P2ry12	F: GCTTTGTTCCCTTCCACTTTG R: GTGCTCTCCTTCACGTAGAAC	1.17 ± 0.34 (11)	0.66 ± 0.10 (12) *
Adora2b	F: TCCGCTACAGTTTCCACAAG R: TTCTCCAAAAGGCCAGAGC	1.01 ± 0.15 (6)	0.91 ± 0.13 (6)
Chrm3	F: TGCTTCTCTTATGCCAGTGTG R: TGTGTATGGGTCACTGCTATTG	1.03 ± 0.28 (6)	1.26 ± 0.15 (6)

*: $p < 0.05$.